ISSN 0023-1584, Kinetics and Catalysis, 2009, Vol. 50, No. 4, pp. 557–566. © Pleiades Publishing, Ltd., 2009.
Original Russian Text © S.N. Rush, Yu.G. Noskov, T.E. Kron, G.A. Korneeva, 2009, published in Kinetika i Kataliz, 2009, Vol. 50, No. 4, pp. 578–587.

Kinetics and Mechanism of Propene Hydroformylation Catalyzed by Rhodium Complexes with a Diphosphite Ligand

S. N. Rush, Yu. G. Noskov, T. E. Kron, and G. A. Korneeva

United Research & Development Centre, Moscow, Russia

e-mail: RushSN@yrd.ru, NoskovYG@yrd.ru

Received May 27, 2008

Abstract—The kinetics of propene hydroformylation in the presence of the catalytic system $Rh(acac)(CO)_2/nL$ (L = 2,2'-bis[(1,1'-diphenyl-2,2'-diyl)phosphito]-3,3',5,5'-tetra-*tert*-butyl-1,1'-diphenyl, $0.5 < n < 20$) in *para*-xylene at 90°C is reported. At $n \geq 2$, the rate and regioselectivity of the process are independent of the L concentration. The reaction is of positive fractional order with respect to propene and hydrogen and of negative order with respect to CO. The molar ratio between the linear product and the branched product decreases with an increasing CO pressure and increases with an increasing H_2 pressure. The kinetic data are consistent with a process mechanism involving irreversible propene addition to the unsaturated hydride complex HRh(CO)L with the formation of the π-complex $HRh(CO)L(C_3H_6)$. The insertion of coordinated propene into the H–Rh bond of this complex is reversible in the linear aldehyde formation route and is quasi-equilibrium in the branched isomer formation route. The conclusions as to the character of these reaction steps are corroborated by the compositions of the but-1-ene and but-2-ene hydroformylation products.

DOI: 10.1134/S0023158409040132

The homogeneous rhodium catalysts for olefin hydroformylation that contain bulky diphosphite ligands show exceptionally high regioselectivity toward the formation of commercially demanded linear aldehydes [1, 2]. With these catalysts, the molar ratio of the linear product (**I**) to the branched product (**II**) is usually 25–50 or above [3]. It is sufficient for the catalyst to contain a small amount of diphosphite (4–7 mol per mole of Rh [4, 5]) or even an equimolar amount of it [6, 7]. For comparison, with the commercial rhodium triphenylphosphine catalyst, a **I**/**II** ratio of about 10 can be ensured only by using a >150-fold excess of the ligand (11–12 wt % of the reaction mixture [8]). Another interesting feature of the diphosphite catalysts is that they allow linear aldehydes to be obtained selectively from internal unsaturated compounds [9]. The structure of rhodium diphosphite complexes and the mechanism of their catalytic action have been the subject of extensive studies [10, 11]. However, the kinetics of the reaction has been discussed mainly at a qualitative level.

Here, we will attempt to correlate, at a quantitative level, kinetic and mechanistic data for propene hydroformylation (Scheme 1) on rhodium complexes with one of the most popular diphosphite ligands (L).

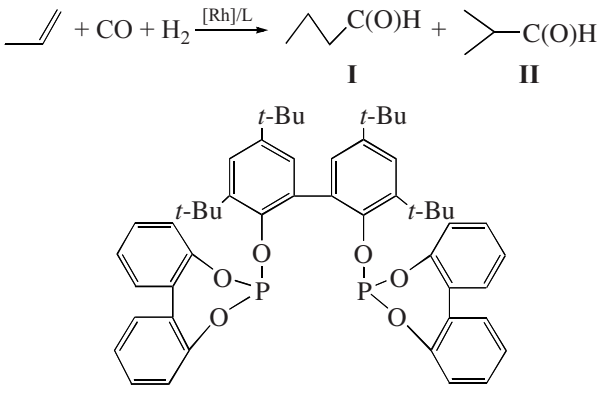

L

Scheme 1.

Table 1. Initial rate (TOF) and regioselectivity (**I/II**) of the hydroformylation reaction at various concentrations of dissolved propene and various partial pressures of hydrogen (P_{H_2}) and carbon monoxide (P_{CO})

Experiment no.	$[C_3H_6]$, mol/l	P_{H_2}, MPa	P_{CO}, MPa	P^*_Σ, MPa	TOF, h^{-1}		**I/II**	
					observed	calculated**	observed	calculated***
1	1.32	0.050	0.050	0.50	13110	12040	9.6	6.9
2	1.32	0.150	0.150	0.70	23500	28270	13.3	15.7
3	1.32	0.300	0.300	1.00	31560	35830	22.3	21.3
4	1.32	0.550	0.550	1.50	33580	32250	24.0	22.3
5	1.32	0.800	0.800	2.00	26815	26480	20.7	20.4
6	1.32	1.300	1.300	3.00	16070	18580	15.7	16.3
7	1.32	1.800	1.800	4.00	12500	14110	13.5	13.3
8	1.32	2.300	2.300	5.00	11000	11320	12.3	11.1
9	1.32	2.800	2.800	6.00	6500	9440	8.3	9.5
10	5.95	0.450	0.450	2.00	76510	76380	22.3	22.5
11	5.95	0.950	0.950	3.00	80270	79590	18.2	19.1
12	5.95	1.450	1.450	4.00	70530	66050	14.4	15.3
13	5.95	1.950	1.950	5.00	49140	54250	11.3	12.6
14	0.365	0.905	0.905	2.00	5000	7290	19.8	19.5
5	1.32	0.800	0.800	2.00	26815	26480	20.7	20.4
15	3.76	0.555	0.555	2.00	67300	64760	22.3	22.2
10	5.95	0.450	0.450	2.00	76510	76380	22.3	22.5
16	1.32	0.200	1.400	2.00	9100	13570	12.3	10.9
17	1.32	0.550	1.050	2.00	16030	20450	17.2	16.6
5	1.32	0.800	0.800	2.00	26820	26480	20.7	20.4
18	1.32	1.050	0.550	2.00	36000	36120	24.6	25.4
19	1.32	1.400	0.200	2.00	69600	70160	39.0	36.9
20	1.32	1.550	0.050	2.00	****	–	44.5	45.4

Note: Reaction temperature of 90°C, *para*-xylene as the solvent, $[Rh] = 3 \times 10^{-4}$ mol/l, L/Rh = 10.

* $P_\Sigma = P_{H_2} + P_{CO} + P_{C_3H_6}$.

** Calculated using Eq. (1) or (5).

*** Calculated using Eq. (2) or (3).

**** The product contains over 10 mol % propane.

EXPERIMENTAL

The diphosphite ligand 2,2'-bis[(1,1'-diphenyl-2,2'-diyl)phosphito]-3,3',5,5'-tetra-*tert*-butyl-1,1'-diphenyl (hereafter, L) was synthesized as described in [12]. ^{1}H NMR ($CDCl_3$, δ, ppm): 1.3 s (36H, *t*-Bu), 6.58 d (2H, Ar), 7.07–7.57 m (18H, Ar).

Hydroformylation was carried in a Parr Instrument high-pressure reactor (0.1 l) fitted with a turbine stirrer (1500 rpm), a pressure gage, and temperature controllers. In a typical experiment (Table 1), the reactor was charged with $Rh(acac)(CO)_2$ (1.55 mg, 0.006 mmol) and the ligand L (50.33 mg, 0.06 mmol) as a *para*-xylene solution (20 ml), purged with nitrogen (1 MPa) four times, and heated to 90°C. Next, the reactor was depressurized to atmospheric pressure and liquid propene (1–12 ml, 12.3–147.6 mmol) was introduced using a doser. The resulting excess pressure was measured, and the amount of the substrate in the gas phase was determined using the ideal gas law. The substrate concentration in the liquid phase was determined as

the difference between the amount of propene charged into the reactor and the amount of propene in the gas phase. The reactor was then filled rapidly with syngas ($CO : H_2 = 1 : 1$) up to a preset pressure, and this instant was taken to be the start time of the reaction. The pressure was maintained constant by replenishing the reactor with syngas from a temperature controlled calibrated vessel via an electronic pressure controller (Brooks Pressure Controller 5866). Syngas uptake data were derived from the pressure drop in the calibrated vessel measured with a pressure sensor connected to a computer, whose readings were taken at 15-s intervals. The reaction rate was determined from the initial portion of the kinetic curve. In experiments 16–20 (Table 1), in which the $CO : H_2$ ratio was varied, the reactor was initially filled with syngas of a preset composition and was then replenished with the $CO : H_2 = 1 : 1$ gas. This could not affect the observed initial rates, because CO and H_2 were consumed in equimolar amounts, according to the stoichiometry of reaction (I).

After the reaction was complete, the reactor was cooled and the reaction mixture was analyzed by GC. The total aldehyde yield was in good agreement with the syngas uptake. The only exception was experiment 20 (Table 1), in which the $CO : H_2$ molar ratio was below 1 : 30 and a considerable amount of propane was formed. In the other runs, the discrepancy was within the error in the gas volume measurements and the uncertainty of the GC analysis (3–5%). Therefore, the hydroformylation kinetics was not affected by side processes and the rate of formation of the aldehydes was equal to the syngas uptake rate. For convenient data comparison, the reaction rate was characterized by the catalyst turnover frequency (TOF) expressed in units of (mol aldehyde) $(\text{mol Rh})^{-1}\,\text{h}^{-1}$ and regioselectivity was characterized by the molar ratio of the products, **I/II**. The regression analysis of kinetic data was carried out using the STATGRAPHICS Plus 5.1 program.

RESULTS AND DISCUSSION

Effects of the Rhodium and Ligand Concentrations

In the presence of excess diphosphite, the reaction is first-order with respect to rhodium. In the rhodium concentration range from 0.1 to 0.8 mmol/l ([L] = 3 mmol/l; the other conditions are the same as in entry 5 in Table 1), the absolute reaction rate increases linearly with increasing [Rh], while the reaction rate in terms of TOF ($\sim 27\,000\ \text{h}^{-1}$) and regioselectivity (**I/II** ≈ 20.5) were invariable within the experimental error. Taking into account this circumstance, we will exclude the dimer complex formation step and the interaction between two rhodium intermediates from the consideration of the process mechanism.

As is demonstrated in Fig. 1, the reaction rate at $L/Rh > 1$ and the regioselectivity of the reaction at $L/Rh \geq 2$ are independent of the ligand concentration. These data are at variance with the data obtained for other diphosphites [11] and monophosphites [13], according to which the reaction rate increases up to the tenfold excess of the ligand. Obviously, the plot shown in Fig. 1 indicates that the full saturation of the coordination sphere of the rhodium atom is reached at $L/Rh \approx 2$, so a further increase in the ligand concentration has no effect on the distribution of rhodium-containing species. However, it is unlikely that the catalytic intermediates are $L/Rh = 2 : 1$ complexes. The results of in situ spectroscopic studies and data concerning the structure of isolated or purposefully synthesized complexes suggest that the intermediates contain a single chelating diphosphite ligand [10, 11, 14, 15]. The monodentate coordination of two diphosphite ligands is unlikely. As distinct from phosphines, monodentate phosphites, which are stronger π-acceptors, apparently do not form 2 : 1 or ligand-richer complexes under hydroformylation conditions [13, 16]. Therefore, the fact that regioselectivity falls sharply as L/Rh is decreased from 2 to 1 (Fig. 1) is most likely due to the formation of species that are low-selective toward isomer **I** and are yet very active. Since the unmodified rhodium catalysts showed an extremely low activity in our experiments ($\text{TOF} = 120\ \text{h}^{-1}$), it is likely that the highly selective chelates are in equilibrium with low-selective dimers (Scheme 2).

The plots presented in Fig. 1 indicate that, even at $L/Rh = 2$, the steady-state concentration of dimers is low and that their contribution to product formation is insignificant. In order to rule out the effect of this factor completely, all subsequent experiments were performed at a tenfold excess of the ligand.

Effect of Temperature

As the temperature is raised from 70 to 100°C, the reaction rate increases by a factor of ~4.5, while the change in regioselectivity does not exceed the experimental error (under the conditions specified in entry 5 in Table 1). The temperature dependence of the rate constant is well linearizable in the Arrhenius coordinates, indicating an apparent activation energy of 54.5 kJ/mol.

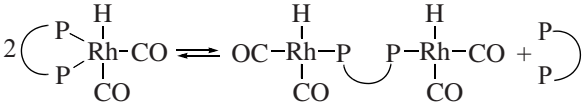

Scheme 2.

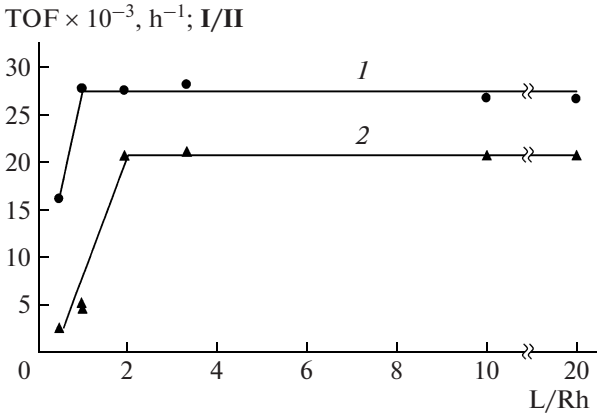

Fig. 1. (*1*) Reaction rate and (*2*) regioselectivity as a function of the L/Rh molar ratio ([Rh] = 0.3 mmol/l; the other conditions are the same as in experiment 5, Table1).

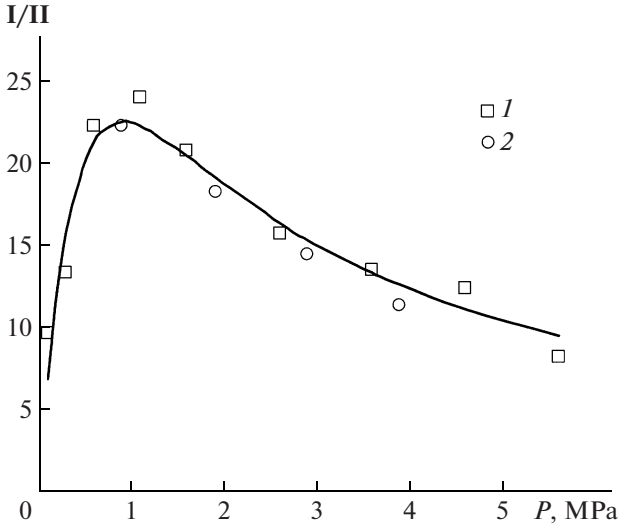

Fig. 2. Regioselectivity (**I/II**) as a function of the syngas pressure (CO : H_2 = 1 : 1). The points refer to propene concentrations of (*1*) 1.3 and (*2*) 5.9 mol/l. The line represents the data calculated using Eq. (2).

Effects of the Concentration and the Partial Pressures of the Reactants

From methodological considerations, kinetic measurements were performed using a multifactorial experiment design. Three series of experiments were carried out: the syngas (CO : H_2 = 1 : 1) pressure was varied at a constant amount of propene, and the amount of propene and the syngas composition were varied at a constant total pressure (Table 1). Thus, the totality of data obtainable in this multifactorial experiment is equivalent to the data that would be obtained in a single-factor experiment if the propene concentration and the CO and H_2 partial pressures were carried separately.

The reaction rate and regioselectivity as a function of the pressure of CO : H_2 = 1 : 1 syngas pass through a maximum near 1 MPa (experiments 1–9). The regioselectivity of the reaction is independent of the propene concentration: the data points obtained for different amounts of the substrate (experiments 1–9 and 10–13) are satisfactorily fitted by one curve (Fig. 2).

The reaction rate increases as the propene concentration is raised. However, raising the substrate concentration at a constant total pressure leads to a decrease in the syngas partial pressure from 1.8 to 0.9 MPa (experiments 5, 10, 14, and 15), causing an increase in the hydroformylation regioselectivity.

At a constant syngas pressure of 1.6 MPa, raising the hydrogen content (changing the CO : H_2 ratio from 7 : 1 to 1 : 7) causes a steady increase in the reaction rate and regioselectivity (experiments 5 and 16–19). As syngas is further enriched with hydrogen (up to CO : H_2 = 1 : 31), the regioselectivity of the process continues to increase, but it becomes impossible to determine the reaction rate reliably because of intensive propene hydrogenation into propane (experiment 20).

By regression analysis of the data presented in Table 1, we constructed an empirical kinetic model. At optimal values of the parameters A_i, this model describes the dependences of the reaction rate and regioselectivity on the concentration of dissolved propene and on the CO and hydrogen partial pressures with a mean relative error of 12 and 6%, respectively. These errors are quite comparable with the mean errors in the measurements of TOF (7–10%) and **I/II** (3–5%). A comparison between the calculated and experimental data is presented in Table 1. The adequacy of the model is graphically illustrated in Fig. 3. Note that the other variants of Eqs. (1) and (2) with statistically significant parameters A_i fit the observed kinetic data much worse.

$$\mathrm{TOF} = \frac{A_1 P_{H_2}[C_3H_6]}{P_{H_2} + A_2 P_{H_2} P_{CO} + A_3[C_3H_6]}, \quad (1)$$

$$\mathrm{I/II} = \frac{A_4 P_{H_2}}{P_{H_2} P_{CO} + A_5 P_{H_2} + A_6}, \quad (2)$$

where $A_1 = 1.74 \times 10^5$ l mol^{-1} h^{-1}, $A_2 = 8.22$ MPa^{-1}, $A_3 = 0.6695$ MPa l mol^{-1}, $A_4 = 32.5$ MPa, $A_5 = 0.531$ MPa, and $A_6 = 0.208$ MPa^2.

These kinetic relationships are very similar to those established for oct-1-ene hydroformylation in the presence of diphosphite **III** (toluene, 60°C, **III**/Rh = 10) [11]. However, no mathematical expressions like Eqs. (1) and (2) were presented in that work.

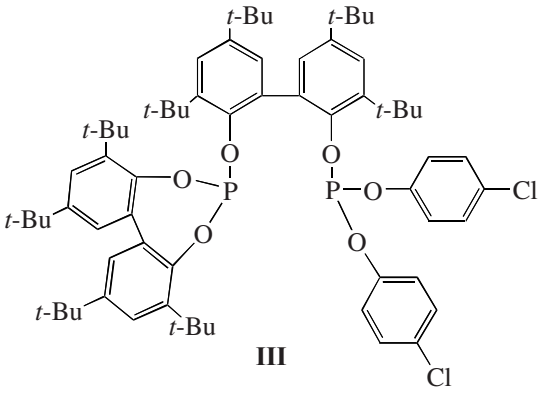

III

In the single-factor experiment reported in [11], in which the oct-1-ene concentration was varied between 0 and 1 mol/l and the CO and H_2 partial pressures were varied between 0.5 and 4 MPa relative to the point with the coordinates $[C_8H_{16}] = 1$ mol/l, $P_{CO} = 1$ MPa, and $P_{H_2} = 1$ MPa, it was found that the reaction rate is first-order with respect to the substrate, has a negative order of –0.65 with respect to carbon monoxide, and is almost independent of the hydrogen pressure (has a formal order of about 0.2). As the CO pressure was raised from 0.5 to 4 MPa, the regioisomer ratio **I/II** decreased from 29 to 4. Our simulation of the experiment in terms of Eqs. (1) and (2) in the same parameter ranges as in [11] gave qualitatively the same results: the formal orders with respect to the substrate, CO, and hydrogen were found to be 0.97, –0.85, and 0.06, respectively; as P_{CO} was raised from 0.5 to 4 MPa, the **I/II** ratio decreased from 26 to 6. Therefore, the propene and oct-1-ene hydroformylation processes in the presence of the structurally similar phosphites L and **III** proceed via similar, if not identical, mechanisms.

Mechanism of the Process

It was reliably demonstrated by IR and NMR spectroscopy that, in the presence of diphosphites, the catalytic precursor $Rh(acac)(CO)_2$ under the action of syngas turns rapidly into a coordinatively saturated hydride complex with the chelating ligand L ($HRh(CO)_2L$ (**IV**)) [11]. Therefore, the process proceeds according to the conventional scheme, which includes the following consecutive steps: alkene coordination with the hydride complex; the addition of the coordinated alkene at the H–Rh bond, yielding a σ-alkyl complex; CO insertion into the C–Rh bond; and the hydrogenolysis of the acyl intermediate. Alkene coordination is likely preceded by the elimination of the carbonyl ligand from complex **IV** with the formation of the catalytically active, unsaturated complex HRh(CO)L (**V**). This is, likely, the cause of the negative order of the reaction with respect to CO. Accordingly, CO insertion into the σ-alkyl complex must not exert any effect on the overall process rate. This is possible when the formation of the σ-alkyl complex includes an irreversible step (Scheme 3, mechanism a) or irreversible spontaneous insertion of a CO ligand into the C–Rh bond of this intermediate takes place to yield a highly unsaturated 14-electron acyl species (Scheme 3, mechanism b).

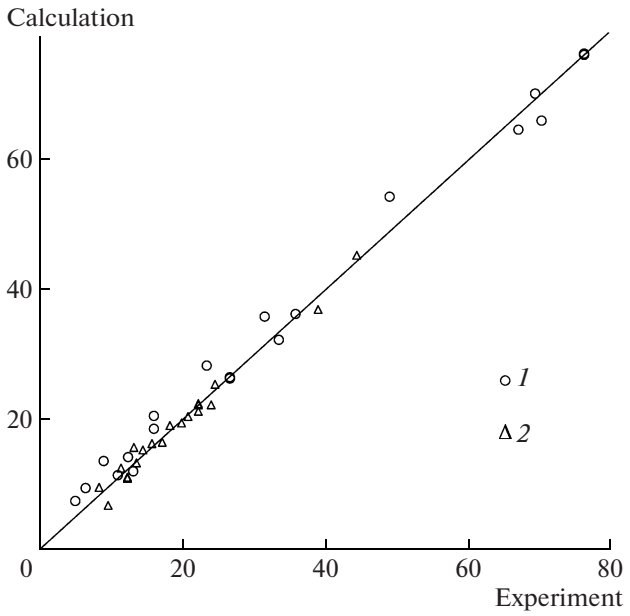

Fig. 3. Comparison between experimental data and data calculated using Eqs. (1) and (2) or Eqs. (3) and (5): (*1*) reaction rate (TOF × 10^{-3}) and (*2*) regioselectivity (**I/II**). The slope of the straight line is 1.0.

At the same time, the negative order of the reaction with respect to CO can be a consequence of the formation of the complex $HRh(CO)_3L$ (with L coordinated in the monodentate mode), another inactive form of the catalyst, which results from the action of CO on the inactive complex **IV** (Scheme 3, mechanism c). In this case, the assumption that the reaction rate is independent of CO insertion into the σ-alkyl complex is unnecessary. Ligand L dissociation or association will not be considered because, under the experimental conditions examined, at L/Rh = 10, the kinetics of the process is independent of the diphosphite concentration (Fig. 1).

In Scheme 3, the steps designated by a single arrow are assumed to be irreversible and the others are considered to be quasi-equilibrium (π-complexes are not shown for simplicity). Under this assumption and under the condition that the material balance for the catalyst includes only the complexes set in bold type (the concentrations of the other complexes are negligible), the mechanisms in Scheme 3 in the steady-state approximation for the catalytic intermediates lead to kinetic equations absolutely identical to Eq. (1). However, as will be demonstrated below, only the modified mechanism (Scheme 3a) provides a rational explanation for the fact that regioselectivity (**I/II**) varies with the CO and hydrogen partial pressures according to Eq. (2).

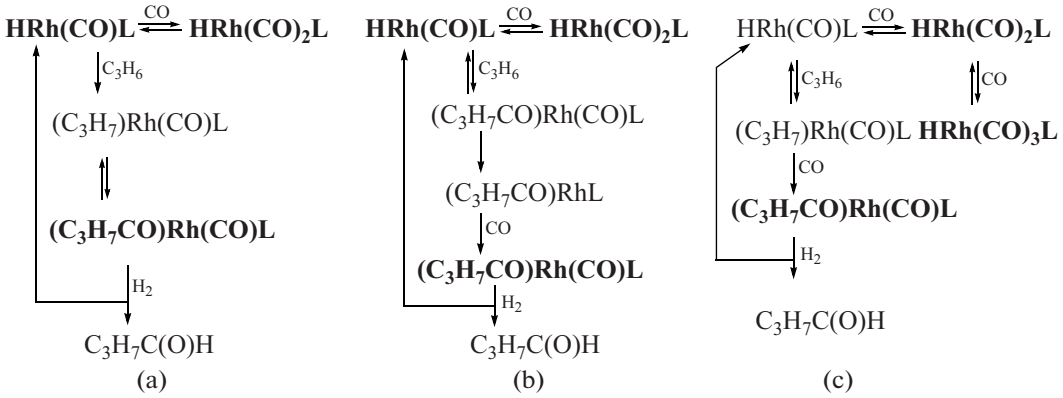

Scheme 3.

In alkene hydroformylation in the presence of rhodium phosphine complexes, the decrease in **I/II** caused by an increasing CO pressure is conventionally attributed to the shift of the equilibrium between the complexes $HRh(CO)(Ph_3P)_3$ and $HRh(CO)_2(Ph_3P)_2$, of which only the former is a source of coordinatively unsaturated hydride species that are highly selective toward isomer **I** (**I/II** increases with an increasing $[Ph_3P]$). The attempts to explain the effect of an increasing CO pressure in the case of the diphosphite complexes in the same way [10, 11] seem groundless. If CO completely replaced the diphosphite in the $HRh(CO)_2L$ complex to yield unmodified hydrides low-selective toward isomer **I**, an increase in [L] would shift the equilibrium in the backward direction. In fact, around L/Rh = 10, the **I/II** ratio depends strongly on the syngas pressure and composition (experiments 1–9 and 16–20 in Table 1), but the L concentration has no effect on the kinetics of the reaction (Fig. 1). If the addition of CO yielded a complex with monodentately coordinated L, such as $HRh(CO)_3L$, this saturated species would hardly be capable of reacting directly with the alkene and the elimination of the CO ligand would immediately restore the highly selective bidentate structure. The change in regioselectivity could be explained by alk-1-ene isomerization into internal olefins [10, 11], but propene does not allow such isomerization.

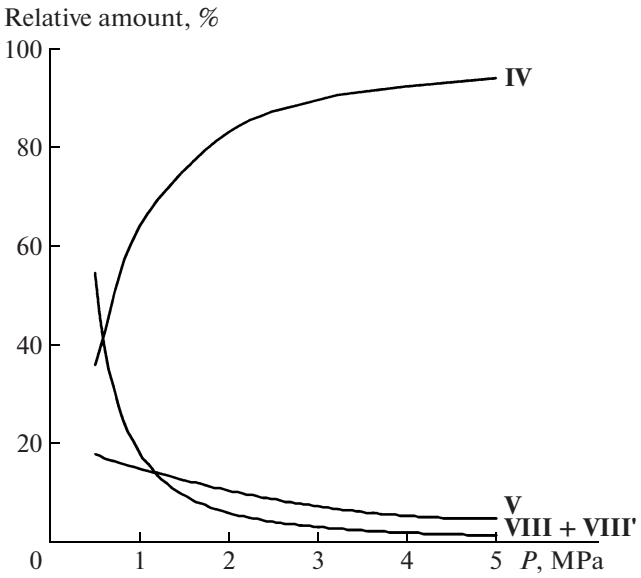

Fig. 4. Calculated dependences of the relative amounts of rhodium complexes on the syngas pressure (CO : H_2 = 1 : 1). The concentration of dissolved propene is 1 mol/l.

In our opinion, the effects of the reaction parameters on the regioselectivity of hydroformylation in the presence of the diphosphite complexes are due to the different characters of the elementary steps in the linear and branched isomer formation routes (Scheme 4).

According to Scheme 4, the structure of the final product is determined by the direction of the insertion of the coordinated alkene into the H–Rh bond in π-complex **VI**, which is the common intermediate for the formation of the linear isomer (route N^1) and the branched isomer (route N^2). Under certain conditions, changes in the concentrations of dissolved CO and hydrogen, which are involved in the subsequent carbonylation of σ-alkyl intermediates and hydrogenolysis of acyl intermediates, can change the ratio between the rates of the reactions via the routes N^1 and N^2. If it is assumed that the formation of linear σ-alkyl complex **VII** (step *2*) is reversible and that the formation of branched complex **VII'** (step *2'*) is quasi-equilibrium, then, if step *3'* is irreversible, it will be possible to express the isomer ratio **I/II** in terms of the constants of elementary steps in Scheme 4 as Eq. (3), which is identical to the empirical equation (2):

$$\mathbf{I/II} = \frac{\frac{k_2}{K_{2'}k_{3'}}P_{H_2}}{P_{H_2}P_{CO} + \frac{k_{-2}}{k_3}P_{H_2} + \frac{k_{-2}k_{-3}}{k_3k_4}}, \quad (3)$$

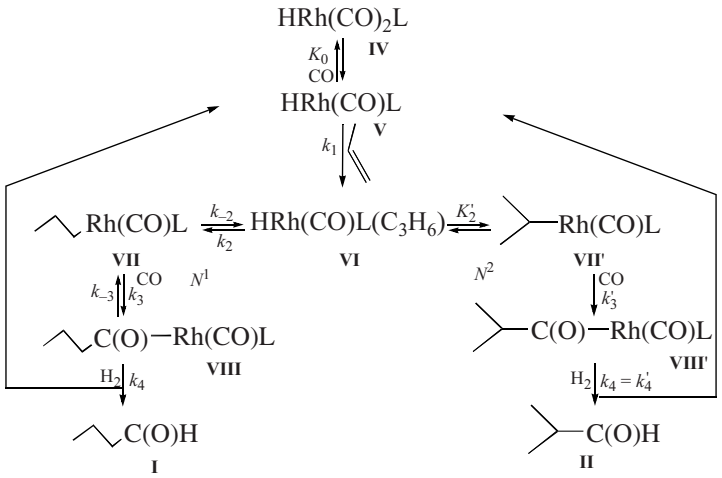

Scheme 4.

where $k_2/(K_{2'}k_{3'}) = 32.5$ MPa, $k_{-2}/k_3 = 0.531$ MPa, $k_{-3} = 1.02 \times 10^5$ h^{-1}, and $k_4 = 2.60 \times 10^5$ MPa^{-1} h^{-1}.

Note that step *3'* in the route N^2, like step *3* in the route N^1 can be viewed as reversible. This complicates Eq. (3) without significantly enhancing the goodness of fit to the observed **I**/**II** data. Complex **VI** can have several structural isomers, for example, **VIa** and **VIb** (Scheme 5). However, under the assumption that the rate of their interconversion is higher than the rate of their conversion into σ-alkyl intermediates, isomers **VIa** and **VIb** can be treated as one species.

In the framework of Scheme 5, the quasi-equilibrium character of step *2'* means that the rate of the decomposition of σ-alkyl intermediate **VII'** to π-complex **VI** (β-elimination of hydrogen) is much higher than the rate of carbonylation into acyl intermediate **VIII'**. The similar step *2* in the route N^1 is reversible: the carbonylation and hydrogen β-elimination rates for complex **VII** are comparable. It is this difference between the reactivities of the two σ-alkyl intermediates that is responsible for the effects of the reaction parameters on the regioselectivity of the process.

For describing the rate of the reaction in terms of an empirical equation like Eq. (1), it is necessary and sufficient to accept that the formation of π-complex **VI** (step *1*) is irreversible and to include the hydride and acyl intermediates in the material balance for the catalyst (Eq. (4)), taking the concentrations of the other species to be negligibly low. It will then be possible to express the hydroformylation rate in terms of the constants of elementary steps in scheme (IV) (Eq. (5)). For simplicity, the hydrogenolysis rate constants of intermediates **VIII** and **VIII'** will be taken to be equal.

$$[\mathrm{Rh}]_0 = [\mathbf{IV}] + [\mathbf{V}] + [\mathbf{VIII} + \mathbf{VIII'}], \qquad (4)$$

$$\mathrm{TOF} = \frac{k_1 P_{\mathrm{H_2}} [\mathrm{C_3H_6}]}{P_{\mathrm{H_2}} + K_0 P_{\mathrm{H_2}} P_{\mathrm{CO}} + \dfrac{k_1}{k_4}[\mathrm{C_3H_6}]}, \qquad (5)$$

where $k_1 = 1.74 \times 10^5$ l mol^{-1} h^{-1}, $K_0 = 8.22$ MPa^{-1}, and $k_4 = 2.60 \times 10^5$ MPa^{-1} h^{-1}.

The material balance equation (4) reflects the well-known fact that, under hydroformylation conditions, only acyl complexes are detectable along with the hydride species, while the steady-state concentrations of the other rhodium intermediates are too low to be detected reliably [17–19]. According to our calculations, the steady-state concentrations of **VIII** and **VIII'** at syngas pressures below 1 MPa far exceed the concentration of hydride complex **V** (Fig. 4). Therefore, the rate-limiting steps in this pressure range are hydrogenolysis reactions *4* and *4'* (Scheme 4). Above 1 MPa, the concentration ratio of these intermediates is inverse and the rate-limiting step is propene coordination with complex **V** yielding π-complex **VI** (step *1*). Simultaneously, raising the pressure displaces rhodium from the intermediates of the catalytic cycle into the inactive, coordinatively saturated, hydride complex **IV** (Fig. 4). At low pressures, this effect is compensated for by the acceleration of the hydrogenolysis steps and the reaction rate even increases (Table 1, experiments 1–3). When hydrogenolysis stops being the limiting step, the reaction rate begins to decrease (experiments 4–9). It is due to these circumstances

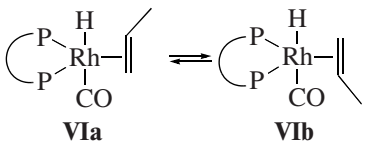

Scheme 5.

Table 2. Hydroformylation of but-1-ene and but-2-ene

Substrate	Composition of the reaction mixture, mol %					**I/II**	TOF**, h^{-1}
	butane*	but-1-ene	but-2-ene	C(O)H **I**	C(O)H **II**		
But-1-ene	2.2	6.4	30.6	58.0	2.8	20.7	25500
But-2-ene	0.7	0.4	63.9	32.3	2.6	12.4	1720

Note: Reaction temperature of 90°C, P_{CO} = 1 MPa, P_{H_2} = 1 MPa, *para*-xylene (20 ml) as the solvent, 0.132 mol of substrate, [Rh] = 1.5×10^{-3} mol/l, L/Rh = 14, reaction time of 1 h.
* Butene hydrogenation product.
** Initial aldehyde formation rate.

that the reaction rate as a function of the syngas ($CO : H_2 = 1 : 1$) pressure passes through an extremum.

The satisfactory agreement between the experimental data and the equations of the above kinetic model (Fig. 3) validates mechanism (**IV**), proving the character of the elementary steps and the catalyst material balance accepted in this mechanism. The assumptions that step *1* is irreversible and that step *2'* is quasi-equilibrium were further verified by an analysis of the product mixture resulting from the hydroformylation of but-1-ene and but-2-ene, the simplest alkenes isomerizing during the reaction (Table 2). In this analysis, we assumed that the amount of any product in the reaction mixture is proportional to the formation rate of this product and that the rate constants of the conversion of similar intermediates in reactions involving butene and propene are equal.

But-1-ene hydroformylation proceeds at nearly the same rate and with nearly the same regioselectivity as propene hydroformylation. A considerable amount of but-2-ene results from this process along with aldehydes. But-2-ene formation is due to the β-elimination of hydrogen from the branched σ-alkyl intermediate **VII'** with the formation of the internal π-complex **VI'**, which then decomposes into rhodium hydride and free but-2-ene (see the step sequence *1*, *2'*, *–2"*, *–1'* in Scheme 6, in which the intermediates and steps analogous to those in propene hydroformylation are designated in the same way as in Scheme 4).

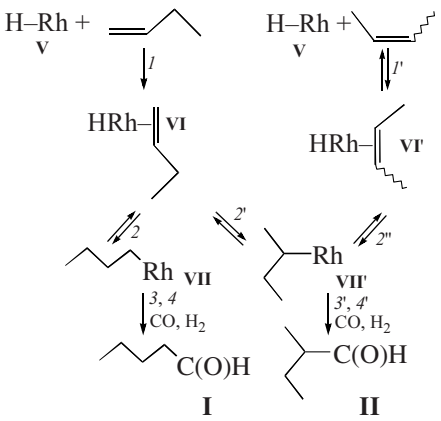

Scheme 6.

The but-2-ene hydroformylation rate is more than one order of magnitude lower than the but-1-ene conversion rate, yet the main product is again a linear aldehyde (**I**). Obviously, this isomer is formed via the β-elimination of hydrogen from the branched σ-alkyl intermediate **VII'** and the formation of the terminal π-complex **VI**, which, as in the case of the route N^1 in Scheme 4, turns into the linear product **I** (step sequence *1'*, *2"*, *–2'*, *2*, *3*, *4*). Notably, the resulting amount of but-1-ene is very small: the **I**/but-1-ene molar ratio is above 80 (Table 2). Therefore, the rate of the conversion of terminal π-complex **VI** into aldehydes is higher than the rate of decomposition of this complex into rhodium hydride and the alkene. This is independent evidence in favor of the irreversibility of the interaction of terminal alkene with hydride species under the hydroformylation conditions, as was assumed in the discussion of step *1* in Scheme 4.

Deuterium exchange studies of the hydroformylation of styrene [20, 21] and hex-1-ene [22] on an unmodified rhodium catalyst demonstrated that the β-elimination of hydrogen from branched σ-alkyl intermediates takes place more intensively than the β-elimination of hydrogen from linear ones. In view of this, there is good reason to assume that the formation of linear complex **VII** in Scheme 4 is reversible and the formation of branched complex **VII'** is a quasi-equilibrium process. According to our calculations, at P_{CO} = 1 MPa the rate of the β-elimination of hydrogen from **VII** is approximately two times lower that the carbonylation rate (see the k_{-2}/k_3 ratio in Eq. (3)). Thus, within the kinetic model discussed

here, these two rates are comparable and, therefore, step *2* is reversible.

A similar ratio between the carbonylation and β-elimination rates for the **VII'**-type branched intermediate can be derived from the composition of the but-2-ene hydroformylation products. Both but-2-ene hydroformylation products— **I** and **II**—are formed via the common intermediate **VII'** (Scheme 6), which is an analogue of the branched σ-alkyl intermediate in Scheme 4. Since practically no but-1-ene formation takes place, the rate of accumulation of the linear product can be expressed in terms of the steady-state concentration of **VII'** using Eq. (6) or the consequential inequality (7). The rate of accumulation of the branched product is given by Eq. (8).

$$r_{\mathrm{I}} = k_{-2'}[\mathbf{VII'}] - k_{2'}[\mathbf{VI}], \quad (6)$$

$$r_{\mathrm{I}} \le k_{-2'}[\mathbf{VII'}], \quad (7)$$

$$r_{\mathrm{II}} = k_{3'}P_{\mathrm{CO}}[\mathbf{VII'}]\,. \quad (8)$$

Under the assumption that the ratio of products in the reaction mixture is equal to the ratio of the formation rates of these products, the following inequality follows from Eqs. (7) and (8):

$$\mathbf{I/II} \le k_{-2'}/(k_{3'}P_{\mathrm{CO}}). \quad (9)$$

From the **I/II** ratio for the reaction involving but-2-ene (Table 2), it can readily be seen that, at $P_{\mathrm{CO}} \approx$ 1 MPa, the constant $k_{-2'}$ is more than 12 times larger than $k_{3'}P_{\mathrm{CO}}$. If the same situation takes place in propene hydroformylation, the β-elimination rate will be higher than the carbonylation rate by the same factor. Therefore, it is quite acceptable to treat step *2'* in Scheme 4 as a quasi-equilibrium reaction.

The simplest explanation of the extremely high regioselectivity (**I/II**) of the rhodium catalysts with bulky bidentate phosphite ligands is that the steric hindrance to the formation of branched σ-alkyl complex **VII'** is greater than the steric hindrance to the formation of linear complex **VII** [10, 11] (see Scheme 4). At the same time, some authors believe that the high regioselectivity is due not to the selectivity of alk-1-ene insertion into the H–Rh bond, but to subsequent reactions [14]. It is also believed that, in the case of bulky ligands, the insertion of CO in branched σ-alkyl complexes can be hampered for a number of steric reasons [23]. As a consequence, **VII**-type linear intermediates turn rapidly into an acyl complexes and then into an aldehyde, while branched intermediates like **VII'**, because of their low carbonylation rate, undergo intensive β-elimination to yield the initial π-complex. This view is supported by the results of this study: the quasi-equilibrium character of the formation of the branched σ-alkyl complexes (Scheme 4, step *2'*) can be due to their low carbonylation rate. Recall that, according to our estimates, the β-elimination-to-carbonylation rate ratio at $P_{\mathrm{CO}} = 1$ MPa at $T = 90°\mathrm{C}$ is ~0.5 for the linear σ-complexes and over 12 for the branched complexes.

From the numerical values of the parameters of Eq. (3), one can readily obtain $K_2k_3/K_{2'}k_{3'} = 61$. The physical meaning of this quantity is regioselectivity (**I/II**) at a CO partial pressure tending to zero and a high hydrogen pressure. The equilibrium constants are measures of the stability of σ-alkyl intermediates **VII** and **VII'** forming from π-complex **VI**, and the rate constants characterize the reactivities of these intermediates at the carbonylation stage. From the kinetic data of this study, it is not absolutely clear which one of the inequalities $K_2 \gg K_{2'}$ and $k_3 \gg k_{3'}$ is responsible for the large **I/II** value. However, the intensive isomerization of but-1-ene and the formation of a linear aldehyde from but-2-ene under our experimental conditions support the latter explanation. It is quite probable that both factors can act simultaneously and which of them is dominant depends on the diphosphite structure. There are highly selective diphosphite catalysts that practically do not cause the isomerization of terminal alkenes into internal alkenes [10, 11]. It is likely that the regioselective effect in this case is mainly due to the suppression of the formation of branched σ-alkyl species upon the insertion of the alkene into the H–Rh bond, whereas the carbonylation rates in the linear and branched product formation routes may be comparable.

REFERENCES

1. US Patent 4769498, 1987.
2. US Patent 4668651, 1985.
3. US Patent 5910600, 1997.
4. US Patent 5202297, 1991.
5. US Patent 5288918, 1992.
6. US Patent 5741945, 1996.
7. US Patent Appl. 2004/0138508 A1, 2004.
8. *Encyclopedia of Catalysis*, Horvath, I.T., Ed., Hoboken, N.J.: Wiley-Interscience, 2003.
9. US Patent 5264 616, 1993.
10. *Catalysis by Metal Complexes*, van Leeuwen, P.W.N.M. and Claver, C., Eds., Dordrecht: Kluwer, 2000, vol. 22.
11. Van Rooy, A., Paul, P.C.J., van Leeuwen, P.W.N.M., Goubitz, K., Fraanje, J., Veldman, N., and Spek, A.L., *Organometallics*, 1996, vol. 15, p. 835.
12. US Patent 5312 996.
13. Van Rooy, A., Orij, E.N.., Kamer, P.C.J., and van Leeuwen, P.W.N.M., *Organometallics*, 1995, vol. 14, p. 34.
14. Moasser, B. and Gladfelter, W.L., *Organometallics*, 1995, vol. 14, p. 3832.
15. Van Rooy, A., Paul, P.C.J., and van Leeuwen, P.W.N.M., *J. Organomet. Chem.*, 1997, vol. 535, p. 201.

16. Van Rooy, A., de Bruijn, J.N.H., Roobeek, K.F., Kamer, P.C.J., and van Leeuwen, P.W.N.M., *J. Organomet. Chem.*, 1996, vol. 507, p. 69.

17. Yagubsky, G., Brown, C.K., and Wilkinson, G., *J. Chem. Soc. A*, 1970, p. 1392.

18. Brown, C.K. and Wilkinson, G., *J. Chem. Soc. A*, 1970, p. 2753.

19. Bianchini, C., Lee, H.M., Meli, A., and Vizza, F., *Organometallics*, 2000, vol. 19, p. 849.

20. Lazzaroni, R., Settambolo, R., Raffaelli, A., Pucci, S., and Vitulli, G., *J. Organomet. Chem.*, 1988, vol. 339, p. 357.

21. Lazzaroni, R., Raffaelli, A., Settambolo, R., Bertozzi, S., and Vitulli, G., *J. Mol. Catal.*, 1989, vol. 50, p. 1.

22. Lazzaroni, R., Uccello-Barretta, G., and Benetti, M., *Organometallics*, 1989, vol. 8, p. 2323.

23. Bronger, R.P.J., Kamer, P.C.J., and van Leeuwen, P.W.N.M., *Organometallics*, 2003, vol. 22, p. 5358.